Numerical Simulation of Hydraulic Turbine During Transient Operation Using OpenFOAM

Numerical Simulation of Hydraulic Turbine During Transient Operation Using OpenFOAM

Saeed Salehi[1], Håkan Nilsson[1], Eric Lillberg[2] and Nicolas Edh[2]

[1] Chalmers University of Technology, Gothenburg, Sweden
[2] Vattenfall AB, Stockholm, Sweden

E-mail: saeed.salehi@chalmers.se

Abstract. Power generation from intermittent renewable energy resources (e.g. wind, solar) requires regulation of the electric grid. Although most hydraulic turbines are designed to work in their best efficiency points, nowadays they are being used more often under varying operating conditions to stabilize the electric grid. Unstable and varying conditions of fluid flow in hydraulic turbines during transient operation cause significant pressure fluctuations and load variations that could negatively affect the turbine lifetime. Therefore, the development of high-fidelity numerical tools for hydraulic turbine flow during transient operation, i.e. changing from one condition to another or during start-up and shut-down, is of great importance for the lifetime prediction of the machines.

In the present work, we are investigating the capabilities of the OpenFOAM open-source CFD tool to predict such phenomena. The transient operation of hydraulic turbines most of the time involves changing the guide vane angles while the runner is rotating, which must thus also be allowed by the employed numerical techniques. The high-head Francis-99 turbine is used as a test case, due to the availability of the geometry and rich experimental data. The turbulence resolving computations are performed using the SAS turbulence model. The numerical results are validated against the experimental data and compared with each other in terms of accuracy and usability. The results are also used for describing the flow behaviors during the shutdown.

1. Introduction

Power production from renewable energy resources is in high demand these days. The inherent intermittency of such resources (e.g. solar or wind) requires special treatment for having constant power output. Nowadays, regulation of the electric grid is mainly done by hydropower. Most modern hydraulic turbines are designed to work at their best efficiency point, and changing their operating condition could generate destructive pressure fluctuations. Therefore, studying the transient phenomena during turbine load changes is very essential.

In this paper, we are studying the transient operation of a Francis turbine during the shutdown procedure. The high-head Francis-99 model turbine is chosen as the investigated test case. The geometry and experimental data are public from the Francis-99 workshop series [**?**].

2. Francis-99 Model Turbine

The Francis-99 model turbine is a 1:5.1 scale model of a prototype Francis turbine located at Tokke power plant, Norway [**?**]. The model is provided by the Francis-99 workshop series as

a test case with rich experimental data to analyze different numerical approaches. Figure 1 presents a three-dimensional view of the Francis-99 turbine assembly. The model consists of four different domains, i.e., spiral casing, guide vanes, runner, and draft tube. It contains 14 stay vanes and 28 guide vanes, while the runner is integrated with 15 splitters and 15 full-length blades. The runner diameter is $D_{\text{runner}} = 0.349$ m. The net head is about $H = 12$ m, calculated as

$$H = \frac{p_1 - p_2}{\rho g} + \frac{v_1^2 - v_2^2}{2g} + z_1 - z_2, \tag{1}$$

where indices 1 and 2 represent spiral casing inlet and draft tube outlet, respectively. The guide vane angle, α, changes between 0.80° and 9.84°, corresponding to minimum load and Best Efficiency Point (BEP), respectively. The guide vane angle is measured with respect to the completely closed position.

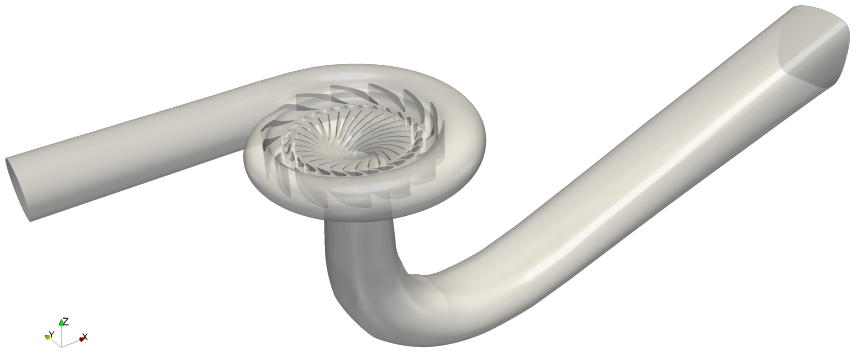

Figure 1: Francis-99 model turbine assembly

During the Francis-99 workshops, a number of measurement locations were determined to compare data between numerical and experimental studies. Three velocity lines, shown in Figure 2, were established for extracting data from the Particle Image Velocimetry (PIV) measurements. Additionally, three different probe locations were chosen for pressure measurements. The locations of the pressure probes are presented in Table 1.

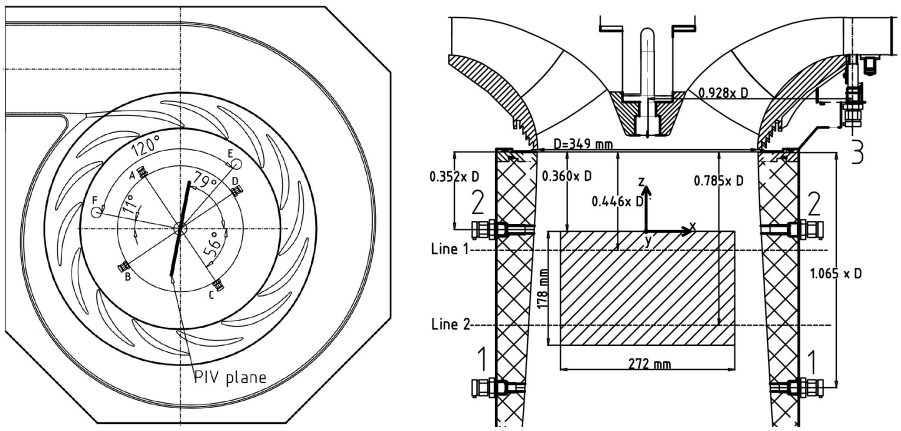

Figure 2: PIV measurement sections in the draft tube [**?**]

Pressure and velocity measurements for a shutdown procedure, from $\alpha = 9.84°$ at BEP to $\alpha = 0.80°$, are available through the Francis-99 web page [**?**]. The transient procedure takes approximately 7 s, during which the runner has a constant speed of 333 rpm and a net head of about 12 m.

Table 1: Pressure probe locations

Probe	VL2	DT5	DT6
x (mm)	-320	-149	149
y (mm)	62	-101	101
z (mm)	-29	-306	-306

3. Computational details

The numerical aspects of the investigated problem, namely, the governing equations of the fluid flow, turbulence modeling, employed numerical methods, and boundary conditions, are elaborated in this section.

3.1. Mathematical formulation

For a transient incompressible turbulent flow, the Reynolds-averaged equations of mass and momentum (also known as Unsteady Reynolds-Averaged Navier-Stokes or URANS) in tensorial form are written as:

$$\frac{\partial U_j}{\partial x_j} = 0, \tag{2}$$

$$\frac{\partial U_i}{\partial t} + \frac{\partial (U_i U_j)}{\partial x_j} = \frac{-1}{\rho}\frac{\partial p}{\partial x_i} + \frac{\partial}{\partial x_j}\left(\nu \frac{\partial U_i}{\partial x_j} - \overline{u_i u_j}\right), \tag{3}$$

where $-\rho\overline{u_i u_j}$ is the unknown Reynolds stress tensor and the system of equations cannot be solved unless this term is identified. In the present study the SST-based Scale-Adaptive Simulation model (SST-SAS model) [**?**] is employed for the calculation of the Reynolds stress tensor, which is a turbulence resolving RANS model, widely used for the simulation of practical transient flows.

3.2. Computational domain and grid

The computational domain is considered from the inlet of the guide vanes to the outlet of the draft tube. Hence three different domains, namely, guide vanes, runner, and draft tube constitute the computational model. The corresponding mesh of each domain is generated separately. First, one passage of guide vane and runner are meshed in Turbo-Grid and ICEM-CFD, respectively. Then the passage is copied and merged to produce the full domains in the ICEM-CFD. The draft tube mesh is also created in ICEM-CFD. The fully structured multi-block meshes are fine enough to resolve the viscous sublayer with low-Reynolds turbulence models. Figure 3 demonstrates some views of the generated mesh for the BEP state.

3.3. Numerical methods and boundary conditions

The CFD computations of the present study were conducted using the finite-volume method with the open-source OpenFOAM-v1912 CFD solver [**?**]. The second-order upwind differencing scheme (`linearUpwind`) was used for discretization of the convective terms in the momentum equation while the upwind (`upwind`) scheme was employed for the k and ω transport equations. Gradient and diffusion terms were interpolated using the central differencing scheme (`linear`). The temporal derivatives were discretized using the Crank-Nicolson scheme [**?**] with a blending factor of 0.5. The time-step of the simulation was chosen as 2×10^{-4}, which corresponds to 0.4° of runner rotation. The mean and maximum Courant-Friedrichs-Lewy (CFL) numbers were around 0.04 and 16, respectively.

The pressure field is linked to the velocity field through the PIMPLE pressure correction algorithm, which combines both SIMPLE and PISO pressure correction algorithms. The PISO

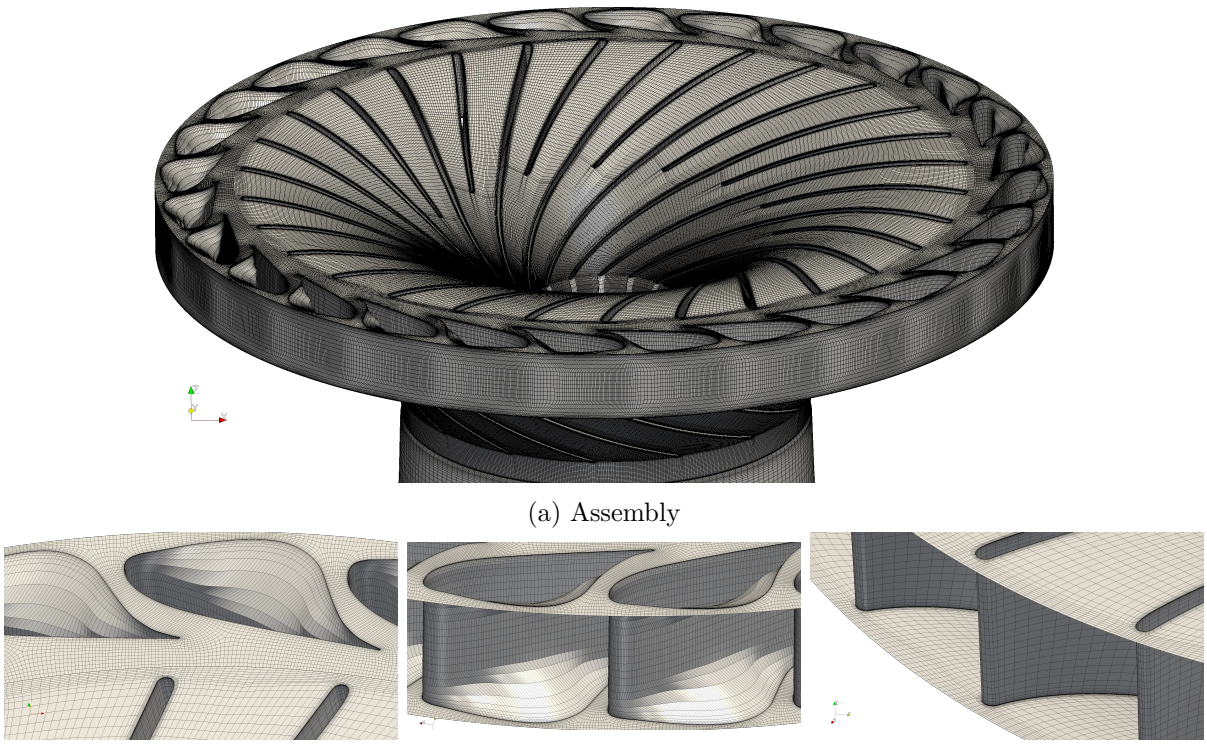

(a) Assembly

(b) Hub

(c) Guide vane blades

(d) Runner blades

Figure 3: Generated computational grid at best efficiency point

is used as an inner loop and SIMPLE as an outer, i.e. a SIMPLE loop was performed on every PISO. PIMPLE was set to operate with PISO loops within every SIMPLE loop and a maximum of 10 SIMPLE loops.

The inlet volume flow rate is assumed to vary with respect to the guide vanes angle. In the Francis-99 turbine shutdown procedure, the guide vanes rotate with a constant rotational speed of $1.3°/s$. Therefore, the inlet flow rate is also assumed to decrease linearly. Figure 4 presents the variation of the guide vane angle and volume flow rate for the shutdown procedure. To avoid numerical instabilities and sudden pressure changes, the starting and stopping processes of the guide vane rotation at $t = 1$s and $t = 8$s occur smoothly using a 5th order polynomial. A new boundary condition for the smooth rotation of the guide vane mesh points is implemented in OpenFOAM.

The inlet flow is supposed to be ideally guided by the upstream stay vanes. In other words, the inflow direction is always parallel to the stay vanes trailing edges. Therefore a time-varying boundary condition is imposed to the radial and tangential velocities in such a way that the volume flow rate always corresponds to the current guide vanes angle, while the flow direction is kept fixed. Additionally, the inlet values of k and ω are also varying with time assuming a fixed turbulence intensity (I) and viscosity ratio (ν_t/ν). The inlet pressure is calculated using a zero-gradient assumption. At the outlet boundary, a zero-gradient condition is imposed for the velocity, while the pressure is assumed to be fixed. The `inletOutlet` boundary type is employed for the treatment of turbulence quantities at the outlet. The boundary type work as a zero-gradient, but it switches to a `fixedValue` type in case of the reversed incoming flow. A no-slip condition is applied for the velocity at the walls, where the turbulent kinetic energy and specific dissipation rate are set to 10^{-8} and the pressure has a zero-gradient assumption.

The non-conformal mesh interfaces between different domains, where the grid points on either

side of the two connected surfaces do not match, need special treatment for computation. In this study the `cyclicAMI` boundary condition is employed for interfaces between guide vane, runner, and draft tube domains. This boundary type transfers data between to mesh surfaces using interpolation based on the algorithm given in [**?**].

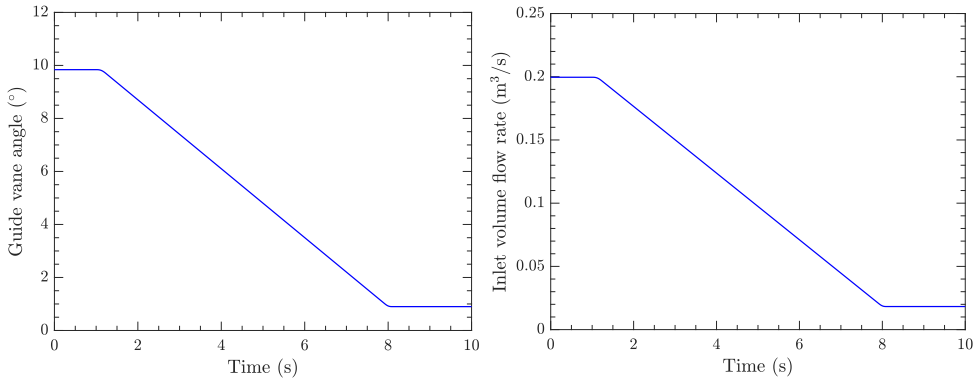

(a) Guide vane angle (b) Volume flow rate

Figure 4: Variation of the (a) guide vane angle and (b) volume flow rate for the shutdown process

3.4. Mesh Motion

In a Francis turbine working in transient operating mode, the guide vanes rotated around their own individual axes, while the runner is also rotating at the same time. Hence, numerical simulation of such flow involves the simultaneous mesh deformation due to guide vanes that change their angle at the same time as the runner part of the computational domain is rotating as a solid body. In order to carry out such simulation, an advanced dynamic mesh tool in OpenFOAM is utilized that enables us to employ different mesh motion solvers on each cell zones. Therefore, a solid body rotation solver is applied on the runner domain, while the Laplacian displacement mesh morphing solver is used for the guide vane domain mesh deformation.

3.4.1. Laplacian Smoothing Mesh morphing through Laplacian smoothing is governed by the

$$\nabla \cdot (\gamma \nabla \boldsymbol{u}) = 0 \tag{4}$$

equation. The motion imposed by the boundary is spread out in the mesh via a diffusivity parameter, γ. The diffusivity may be governed linearly, exponentially, inverse distance to the object or via any arbitrary decreasing function. An inverse distance approach with respect to the guide vane surfaces is employed for the diffusivity, which decreases with distance from the motion. It other words, points close to the moving wall are more affected by the boundary movement than those further away [**?**]. Consequently, the cells close to the moving guide vanes move almost as solid body, while the cells far away from the boundary deform noticeably. $\boldsymbol{u}$ is the velocity field of the points, used to modify points position, $\boldsymbol{x}$, as

$$\boldsymbol{x}_{new} = \boldsymbol{x}_{old} + \boldsymbol{u}\Delta t \tag{5}$$

The motion procedure can be decomposed in a number of steps [**?**]. Firstly, all polyhedral cells are divided into tetrahedral, by splitting faces to triangles, and a cell center point is introduced. The second step is to use the Laplace operator and move points, using equations 4 - 5.

The next step is to perform the motion of the wall by executing the equation of motion prescribed by the boundary condition. The wall displacement, and thus point displacement, is solved in an iterative manner until convergence is reached [**?**].

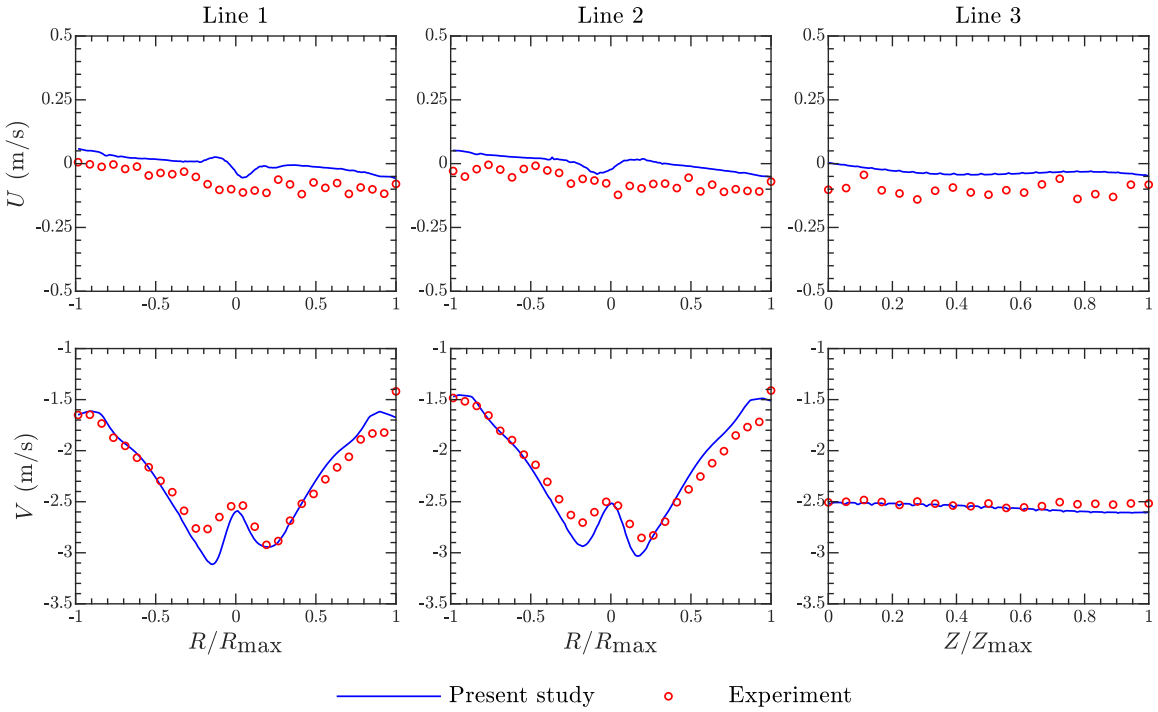

Figure 5: Time-averaged numerical results of horizontal (U) and vertical (V) velocities on different lines compared to experimental PIV data

4. Results and discussion

This section presents the numerical results of the steady and transient shutdown procedure of the Francis-99 turbine compared to experimental measurements.

At first, a steady potential flow is solved as an initial guess and then the transient turbulent simulation is executed to reach a fully developed unsteady condition at the best efficiency operating point. After reaching a statistically stationary state, the simulation is continued for another 1 s flow-time for time-averaging.

4.1. Best efficiency point

The statistically stationary results at the best efficiency operating point, where the guide vanes are kept still, are presented in this section. The runner has a constant rotational speed of 332.58 rpm and the volumetric flow rate is fixed at $Q_{\mathrm{BEP}} = 0.19959$ m^3/s.

Time-averaged numerical results of the SAS turbulence model for both the vertical (axial) and horizontal velocities are presented and compared to measured PIV data in Figure 5. It should be recalled that the location of the PIV measurement plane was previously shown in Figure 2. The comparison reveals an acceptable agreement between the numerical results and the experimental data. The decrease of axial velocity close to the rotational axis, caused by the wake behind the flat surface of the runner at the center, is well captured by the numerical results.

4.2. Shutdown

In this section, the transient results for the shutdown procedure are presented and discussed. As mentioned before, the guide vane mesh motion is activated after reaching statistically stationary state at the best efficiency point. The guide vanes rotate according to the prescribed time-varying boundary condition in Figure 4a. The corresponding mesh is morphed in each time

step by solving the Laplacian displacement equation and updating the location of all points in the domain. Due to the mesh quality considerations, the guide vane domain mesh cannot be morphed all the way from the best efficiency point down to the fully closed position. So the mesh is reproduced whenever the quality is low, causing numerical instabilities. Subsequently, the results are interpolated between the previously morphed mesh and the new one and the solution continues. Figure 6 illustrates the unmorphed best efficiency point guide vane mesh ($\alpha = 9.84$) as well as rotated guide vanes with morphed meshes at two sections. It should be recalled that the guide vane angles are calculated with respect to the fully closed position.

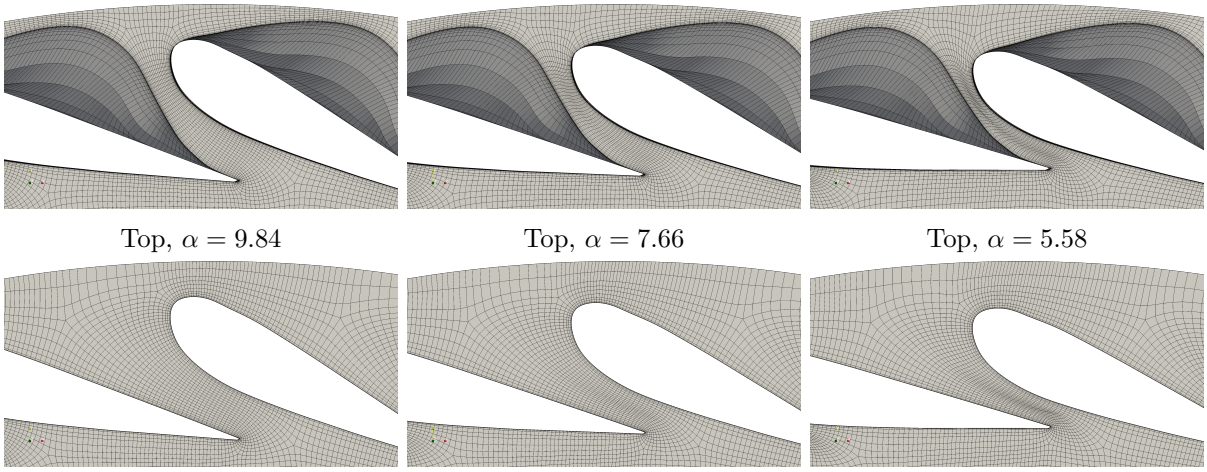

Figure 6: Visualization of mesh morphing on the top and middle planes of the guide vane domain

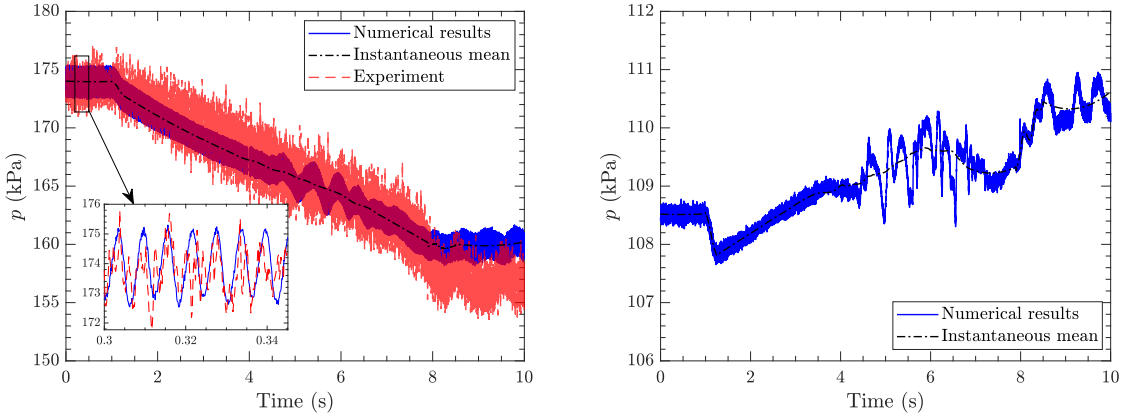

(a) VL2 (b) DT5

Figure 7: Static pressure in two probes during shutdown

4.3. Pressure Probes

Numerical and experimental transient pressure data for the VL2 (vanless space) and DT5 (draft tube) probes are displayed in Figure 7 during the shutdown procedure. It should be mention that in the experimental studies the VL2 pressure probes measured the static pressure, while the DT5

and DT6 probes were piezo-electric type dynamic sensors and thus measured the only pressure fluctuations. In general, the numerical results of the present study are in good agreement with the experimental data. The pressure is slightly over-predicted during the minimum load phase ($t > 8$ s). The VL2 static pressure shows when the guide vanes movement and flow rate reduction initiate, the pressure starts decreasing with an almost constant rate. After reaching the minimum load the pressure oscillates around a constant rate.

The pressure in the draft tube, presented in Figure 7b,indicates decreasing guide vane angle and incoming flow rate enhances the pressure fluctuations due to the growth of flow unsteadiness in low load conditions.

4.4. Velocity Lines

Contour plots of axial velocity during the shutdown sequence at velocity line 1 are found in Figure 8. It can be seen in both numerical and experimental contours that closing the guide vanes forms a recirculation zone in the center of the draft tube which gets stronger with decreasing flow rate at lower turbine loads.

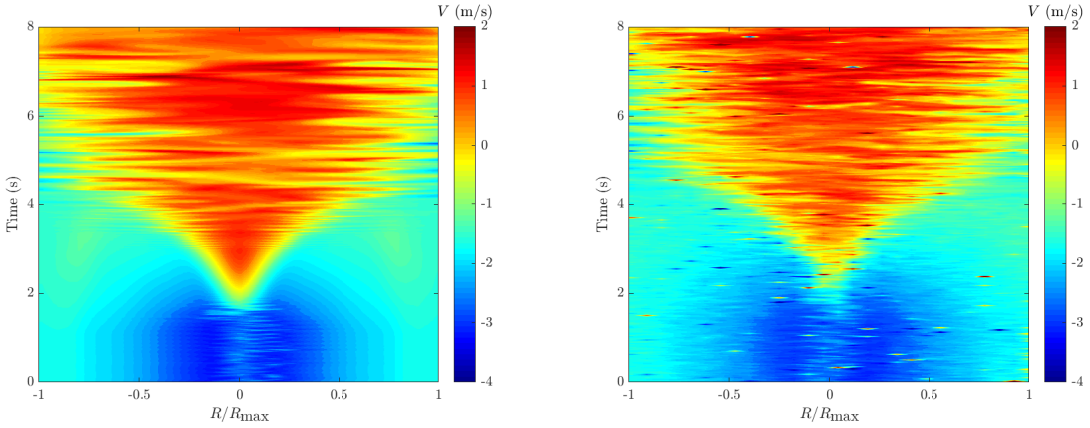

(a) Simulated (b) Experimental

Figure 8: Contour plot of axial velocity during shutdown at line 1. Note that time is displayed on the y-axis and that the figure is read from bottom to top.

The same trend is seen in the velocity contours of line 2 depicted in Figure 9.

Contours for the axial velocity at the vertical line 3 can be seen in Figure 10. Here also the formation and enhancement of the unsteady recirculation zone below the hub center is visible.

5. Conclusion

The shutdown sequence of the high-head Francis-99 model turbine was numerically investigated in this paper. The CFD simulations were carried out using the open-source CFD tool OpenFOAM. Each guide vanes rotated around its own individual axes, while the runner is also rotating around the turbine axis at the same time. Guide vane domain mesh motion was enabled through the Laplacian displacement mesh morphing solver while a solid body rotation approach was employed for the runner domain. The flow rate of the turbine was assumed to change linearly with the guide vane opening angle. The SAS model was used for turbulence modeling. First, the velocity field in the draft tube was validated against experimental data at the best efficiency point. The vaneless space pressure decreases during shutdown and oscillates at the minimum load. The pressure fluctuations in the draft tube enhance during the shutdown.

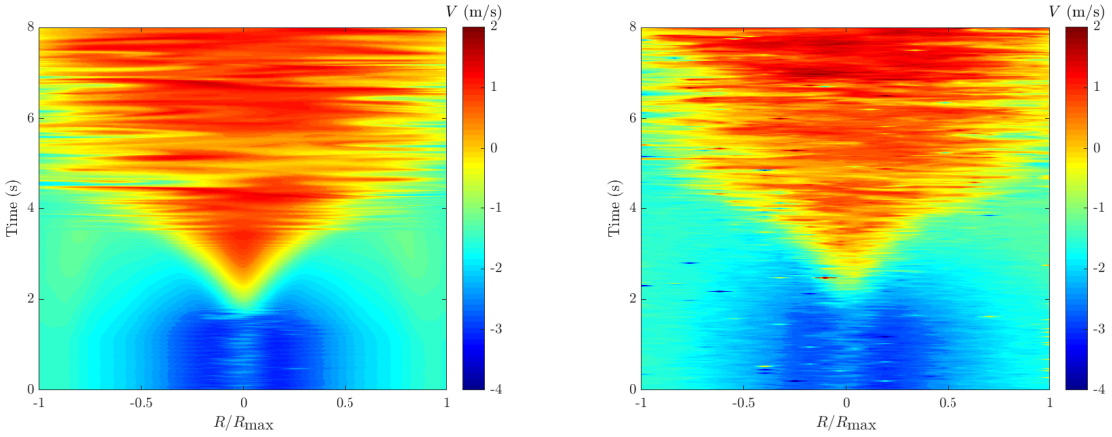

(a) Simulated (b) Experimental

Figure 9: Contour plots of axial velocity during shutdown at line 2. Note that time is displayed on the y-axis and that the figure is read from bottom to top.

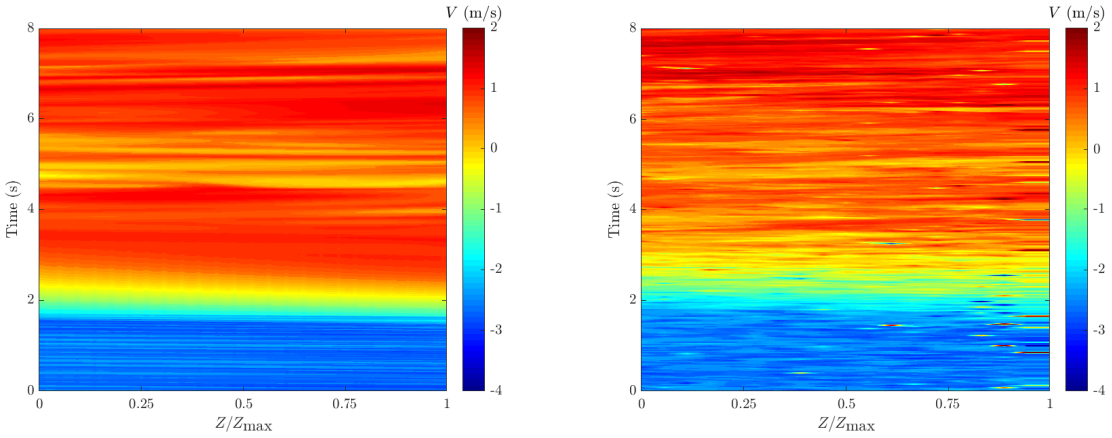

(a) Simulated (b) Experimental

Figure 10: Contour plot of axial velocity during shutdown at line 3. $Z/Z_{max} = 0$ represents the position closest to the runner and $Z/Z_{max} = 1$ the furthest. Note that time is displayed on the y-axis and that the figure is read from bottom to top.

The draft tube velocity field indicates the formation of a recirculation zone in the center of the draft tube which gets stronger with decreasing flow rate at lower turbine loads.

6. Acknowledgements

The research presented was carried out as a part of the "Swedish Hydropower Centre - SVC". SVC is established by the Swedish Energy Agency, EnergiForsk and Svenska Kraftnät together with Luleå University of Technology, The Royal Institute of Technology, Chalmers University of Technology and Uppsala University, www.svc.nu. The computations were enabled by resources provided by the Swedish National Infrastructure for Computing (SNIC) at NSC partially funded by the Swedish Research Council through grant agreement no. 2018-05973.

References